Journal of Power Sources 196 (2011) 4298–4305

Contents lists available at ScienceDirect

Journal of Power Sources

journal homepage: www.elsevier.com/locate/jpowsour

LPV observer design for PEM fuel cell system: Application to fault detection☆

S. de Lira[a,*,1], V. Puig[a,1], J. Quevedo[a,1], A. Husar[b,2]

[a] Sistemas Avanzados de Control (SAC), Universitat Politécnica de Catalunya (UPC), Rambla Sant Nebridi 10, 08222 Terrassa, Spain
[b] Instituto de Robótica i Informática Industrial (IRI), (CSIC-UPC) Parc Tecnológic de Barcelona, Edifici U, Carrer Llorens i Artigas, 4-6, Floor 2, 08028 Barcelona, Spain

ARTICLE INFO

Article history:
Received 31 July 2010
Received in revised form 14 October 2010
Accepted 17 November 2010
Available online 25 November 2010

Keywords:
PEM fuel cell
Modelling
LPV
Observer
Fault detection

ABSTRACT

In this paper, the modelling of an energy generation system based on *polymer electrolyte membrane fuel cell* (PEMFC) system through a parameter varying approach (LPV model), that takes in to account model parameter variation with the operating point, is presented. This model has been obtained through a Jacobian linearization of the PEMFC non-linear dynamic model that was previously calibrated using real data from lab. In order to illustrate the use of the LPV model obtained its application to model-based fault detection is used. For this purposes a set of common fault scenarios, which could appear during a normal PEMFC operation, is used as case study.

© 2010 Elsevier B.V. All rights reserved.

1. Introduction

Low-temperature PEM fuel cells are considered as sources for rapid medium of energy generation, making these equipment suitable for automobile applications. The supply of raw materials (usually air or pure oxygen) is normally performed using an air compressor or blower and hydrogen stored in tanks. The system uses additional equipment to carry materials reaction to the optimum operating conditions, such as cooling systemsand humidifier. During the chemical reaction that is taking place into the stack, where the energy is generated, different phenomena occur, such as thermal, fluid-mechanical and electrolytic.

The complex and non linear dynamics of the power generation systems based on fuel cell technology lead to the use of linear models that includes parameter varying with operating point not only for advanced control techniques but also for fault diagnosis algorithms based on models. The use of LPV models is an alternative to the approaches presented in previous works [1,2] addressing methodologies for monitoring and fault diagnosis based on a theoretical non-linear dynamic model proposed by Pukrushpan [3,4].

Within the recent decade, state of art and background about control of LPV systems has been developed [5–10]. Because of a LPV system can be considered as a parametrized family of linear systems that change with the operating point conditions, then LPV technique allows a systematic approach for control and fault diagnosis system design. At the cost of conservatism the approach can be applied to an even wider range of systems known as quasi-LPV systems, where varying parameters are scheduled with state variables.

Since LPV models are structured as similar as a linear time-invariant (LTI) state space system, the control and fault diagnosis design methods can easily be extended. The main contribution of this paper is to obtain a linear parameter varying model for a typical PEMFC and illustrate its use for robust fault detection using interval observers.

2. Fuel cell modelling

The model proposed in [11], is a non-linear dynamic model calibrated using real data from laboratory using a *lsq*-non linear fitting approach [12,13]. This model is able to reproduce the behaviour of a commercial PEMFC (Ballard 1.2 kW, Nexa©) prototype, which has been identified in a wide range of operating conditions. Fig. 1 shows the dynamic model layout.

2.1. Dynamic non-linear model

The model is considered as SIMO system, where the input (u) is the stack current (I_{st}) and the outputs (y) are battery temperature (T_{st}), stack voltage (v_{st}), oxygen consumption ratio (λ_{O_2}), speed

☆ This work has been partially funded by the grant CICYT HYFA DPI2008-01996 of Spanish Ministry of Education and by a grant from Consejo Nacional de Ciencia y Tecnologia (CONA-CyT), México. The authors wish also to thank to the Instituto de Robotica i Informatica Industrial (IRI/UPC-CSIC) for its know how sharing, specially to J. Riera, M. Serra and D. Feroldi.

* Corresponding author. Tel.: +34 622111233; fax: +34 934015750.
E-mail address: salvador.de.lira@upc.edu (S. de Lira).
[1] http://websac.upc.es.
[2] http://www.iri.upc.edu.

0378-7753/$ – see front matter © 2010 Elsevier B.V. All rights reserved.
doi:10.1016/j.jpowsour.2010.11.084

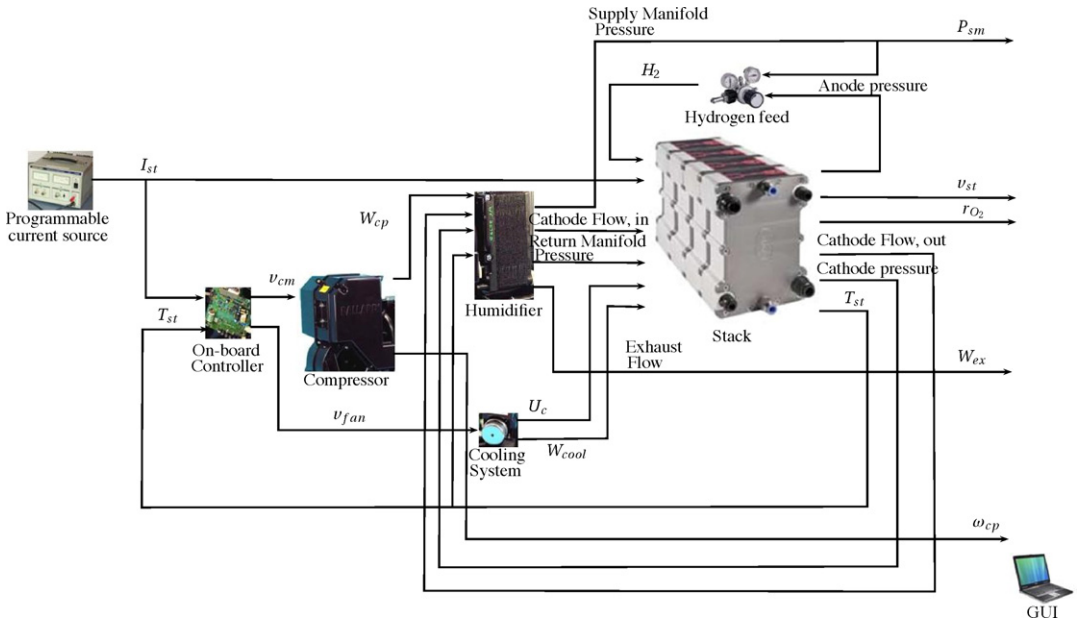

Fig. 1. Nexa© PEMFC simulator schematic.

engine (ω_{cp}) and inlet pressure to the cathode (P_{sm}). The voltage from the compressor (v_{cm}) is controlled using a static feed-forward controller. Fig. 2 shows the layout of each subsystem embedded into the PEMFC dynamic model.

The proposed model consists often state, and the state equations are listed in the following

$$\begin{aligned}
\dot{\omega}_{cp} &= \frac{1}{J_{cp}\omega_{cp}}(\tau_{cm} - \tau_{cp}),\\
\dot{P}_{rm} &= \frac{R_{air}T_{rm}}{V_{rm}}(W_{ca,o} - W_{rm,o}),\\
\dot{m}_{rm} &= W_{ca} - W_{rm,o},\\
\dot{P}_{sm} &= \frac{\gamma R_a}{V_{sm}}(W_{cp}T_{cp} - W_{sm,o}T_{sm}),\\
\dot{m}_{sm} &= W_{cp} - W_{sm,o},\\
\dot{m}_{H_2} &= W_{H_2,i} - W_{H_2,o} - W_{H_2,r-W_{H_2,nl}},\\
\dot{m}_{w,an} &= W_{v_{an},i} - W_{v_{an},o} - W_{v_{mbr}},\\
\dot{m}_{N_2} &= W_{N_2,i} - W_{N_2,o},\\
\dot{m}_{O_2} &= W_{O_2,i} - W_{O_2,o} - W_{O_2,r},\\
m_{st}C_{st}\dot{T}_{st} &= H_{reac} - P_{elec} - Q_{rad} - \dot{Q}_{conv}.
\end{aligned} \tag{1}$$

The state variables ($\mathbf{x}$) of this dynamic model are the following: mass of oxygen (m_{O_2}), nitrogen (m_{N_2}), hydrogen (m_{H_2}), cathode water flow ($m_{w,ca}$), stack temperature (T_{st}), angular velocity of the compressor (ω_{cp}), supply pressure (P_{sm}) and return pressure (P_{rm}) of the humidifier, inlet flow (m_{sm}) and outlet flow (m_{rm}) of humidifier. The subindex in the variables *i*, *o*, *r*, *nl* means, input, output, reaction and natural, respectively. In the heat balance the subindex *reac*, *elec*, *rad* and *conv* are related respectively to reaction, electric, radiation and convection.

The system perturbation ($\mathbf{z}$) that have been considered are related to the weather conditions (T_{amb}, P_{atm}).

The model output equations are:

- *Stack voltage*:

$$v_{st} = n_{fc}\cdot(E - v_{act} - v_{oh} - v_{con}). \tag{2}$$

- *Oxygen excess ratio*:

$$\lambda_{O_2} = \frac{W_{O_2,i}}{W_{O_2,r}} = \frac{x_{O_2}\cdot W_{cp}}{(M_{O_2}\cdot n_{fc}\cdot I_{st})/4\cdot F}. \tag{3}$$

- *Compressor speed motor*:

$$\omega_{cp} = \frac{U_{cp}\cdot 60}{d_c\cdot\pi}, \tag{4}$$

where v_{st}, total stack voltage (V); E, open circuit voltage (V); v_{act}, activation voltage loss (V); v_{oh}, ohmic voltage lose (V); v_{con}, concentration voltage loss (V); n_{fc}, amount of cells; λ_{O_2}, oxygen excess ratio; I_{st}, stack current (A); F, Faraday constant (col/mol); W, mass flow (g/s); U_{cp}, compressor blade (KRPM); d_c, compressor diameter blade (%); η, compressor efficiency (%); M_{O_2}, oxygen molar weight (g/mol); M_{H_2}, hydrogen molar weight (g/mol); x_{O_2}, oxygen fraction (%); φ_i, humidity ($i = ca, an$) (%).

3. Linear parameter varying model

Exist different ways to obtain LPV models. Some methods use non-linear equations of the system to derive a LPV model such as state transformation, substitution of functions and methods using the well known Jacobian linearization [14–16]. Another kind of method uses multi-model identification that consists basically in two different steps: (1) a set of LTI model is identified at different equilibrium points by classical methods (*on-line* or *off-line*), (2) then, the following step is to get a multi-model by an interpolation law that allows to commute among local LTI model at each operating point [17,18].

3.1. Problem formulation

The type of LPV system, which is considered in this paper, assumes an affine dependence with a parameter vector $\tilde{\vartheta}_k$ and can be described in discrete time state space as:

$$\begin{aligned}
\mathbf{x}_{k+1} &= \mathbf{A}(\tilde{\vartheta}_k)\mathbf{x}_k + \mathbf{B}(\tilde{\vartheta}_k)\mathbf{u}_k + \mathbf{w}_k,\\
\mathbf{y}_k &= \mathbf{C}(\tilde{\vartheta}_k)\mathbf{x}_k + \mathbf{D}(\tilde{\vartheta}_k)\mathbf{u}_k + \mathbf{v}_k,
\end{aligned} \tag{5}$$

where $\mathbf{x}_k \in \mathbb{R}^{n_x}$, $\mathbf{u}_k \in \mathbb{R}^{n_u}$ and $\mathbf{y}_k \in \mathbb{R}^{n_y}$ are, respectively, the state, input, and output vectors. The process and measurement noises are $\mathbf{w}_k \in \mathbb{R}^{n_x}$ and $\mathbf{v}_k \in \mathbb{R}^{n_y}$ respectively. Both are considered unknown but bounded as $\mathbf{v}_k \in \mathbb{V}^{n_x}$ and $\mathbf{w}_k \in \mathbb{W}$ which are interval boxes.

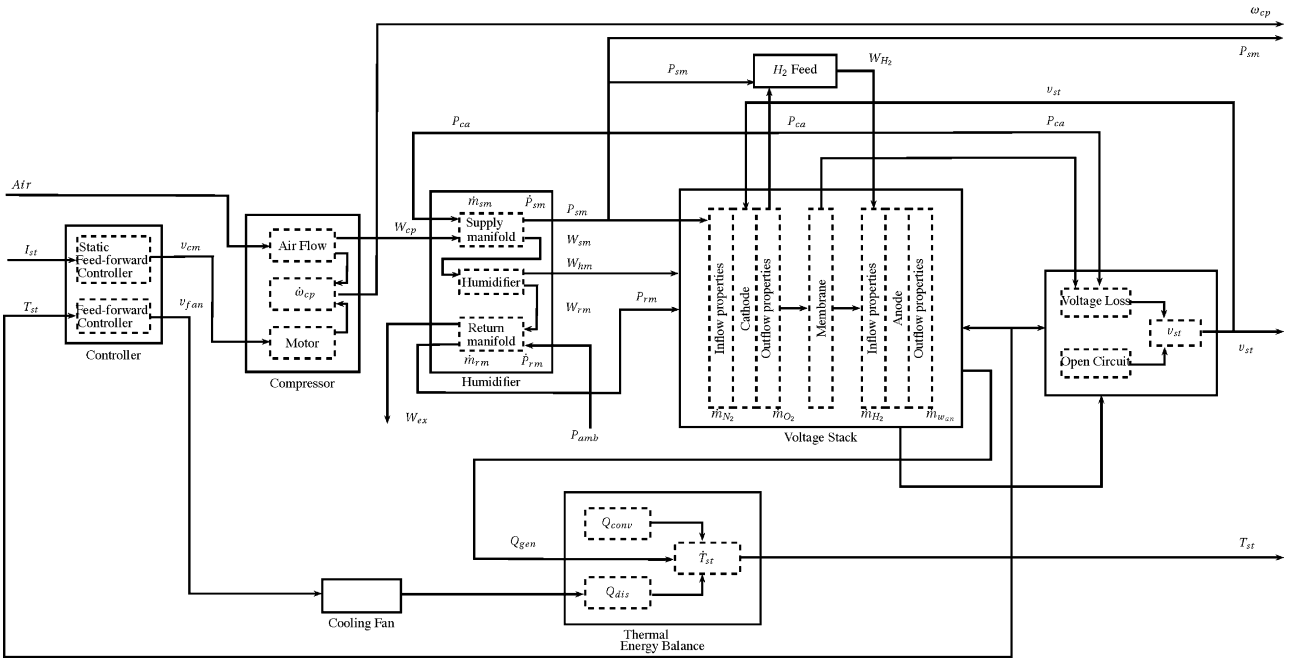

Fig. 2. Nexa© PEM fuel cell dynamic model diagram.

$\tilde{\vartheta}_k \in \Theta$ is the vector of time-varying parameters that change with the operating point scheduled by some measured system variablesp_k ($p_k := p(k)$) that can be estimated using some known function:

$$\tilde{\vartheta}_k = f(p_k), \tag{6}$$

where

$$\Theta = \{\tilde{\vartheta}_k \in \mathbb{R}^{n_\vartheta} | \underline{\tilde{\vartheta}}_k \le \tilde{\vartheta}_k \le \bar{\tilde{\vartheta}}_k\}. \tag{7}$$

The system described in Eq. (5) could be seen as a linear model parameterized by a monitored variable through Eq. (7) [5,19,20,21]. In practice, the model in Eq. (6) by a polytope of dimension is N described as an array of matrices described by

$$\begin{aligned}\begin{bmatrix}\mathbf{A}(\tilde{\vartheta}_k) & \mathbf{B}(\tilde{\vartheta}_k)\\ \mathbf{C}(\tilde{\vartheta}_k) & \mathbf{D}(\tilde{\vartheta}_k)\end{bmatrix} &\in \left\{\begin{bmatrix}\mathbf{A}_j(\vartheta^j) & \mathbf{B}_j(\vartheta^j)\\ \mathbf{C}_j(\vartheta^j) & \mathbf{D}_j(\vartheta^j)\end{bmatrix}\right\}\\ &\cong \sum_{j=1}^{N}\alpha_j(p_k)\cdot\begin{bmatrix}\mathbf{A}_j(\vartheta^j) & \mathbf{B}_j(\vartheta^j)\\ \mathbf{C}_j(\vartheta^j) & \mathbf{D}_j(\vartheta^j)\end{bmatrix},\end{aligned} \tag{8}$$

where $\mathbf{A}_j$, $\mathbf{B}_j$, $\mathbf{C}_j$and $\mathbf{D}_j$ are the state matrices for each jth model obtained by linearization of the non-linear model around the jth operating point. Using Eq. (8), the Eq. (5) can be approximated as follows:

$$\begin{aligned}\mathbf{x}_{k+1} &= \sum_{j=1}^{N}\alpha^j(p_k)\cdot[\mathbf{A}_j(\vartheta^j) \quad \mathbf{B}_j(\vartheta^j)]\cdot\begin{bmatrix}\mathbf{x}_k\\ \mathbf{u}_k\end{bmatrix},\\ \mathbf{y}_k &= \sum_{j=1}^{N}\alpha^j(p_k)\cdot[\mathbf{C}_j(\vartheta^j) \quad \mathbf{D}_j(\vartheta^j)]\cdot\begin{bmatrix}\mathbf{x}_k\\ \mathbf{u}_k\end{bmatrix}.\end{aligned} \tag{9}$$

3.2. PEMFC LPV structure

Using the PEMFC non-linear dynamic model presented in Section 2.1 and using the Jacobian linearization approach, the non-linear model is possible to transform it into a LPV model in state space form, as in Eq. (9) with the following system matrices structure

$$\mathbf{A}_j = \begin{bmatrix} a_{11} & 0 & 0 & a_{14} & 0 & 0 & 0 & 0 & 0 & 0\\ 0 & a_{22} & a_{23} & a_{24} & a_{25} & 0 & 0 & a_{28} & a_{29} & a_{210}\\ 0 & a_{32} & 0 & a_{34} & a_{35} & 0 & 0 & a_{38} & a_{39} & a_{310}\\ a_{41} & 0 & 0 & a_{44} & a_{45} & 0 & 0 & a_{48} & a_{49} & a_{410}\\ a_{51} & 0 & 0 & a_{54} & 0 & 0 & 0 & a_{58} & a_{59} & a_{510}\\ 0 & 0 & 0 & a_{64} & 0 & a_{66} & a_{67} & 0 & 0 & a_{610}\\ 0 & 0 & 0 & a_{74} & 0 & a_{76} & a_{77} & 0 & 0 & a_{710}\\ 0 & a_{82} & 0 & a_{84} & a_{85} & 0 & 0 & a_{88} & a_{89} & a_{810}\\ 0 & a_{92} & 0 & a_{94} & a_{95} & 0 & 0 & a_{98} & a_{99} & a_{910}\\ 0 & 0 & 0 & 0 & 0 & a_{106} & a_{107} & 0 & a_{109} & 0 \end{bmatrix},$$

$$\mathbf{C}_j = \begin{bmatrix} c_{11} & 0 & 0 & 0 & 0 & 0 & 0 & 0 & 0 & 0\\ 0 & 0 & 0 & c_{24} & 0 & 0 & 0 & 0 & 0 & 0\\ 0 & 0 & 0 & c_{34} & c_{35} & 0 & 0 & c_{38} & c_{39} & c_{310}\\ 0 & 0 & 0 & 0 & 0 & c_{46} & c_{47} & c_{48} & c_{49} & c_{410} \end{bmatrix},$$

$$\mathbf{B}_j = \begin{bmatrix} b_{11} & b_{12}\\ 0 & 0\\ 0 & 0\\ 0 & 0\\ 0 & 0\\ b_{71} & 0\\ b_{81} & 0\\ 0 & 0\\ b_{91} & 0\\ b_{101} & 0 \end{bmatrix}, \qquad \mathrm{D}_j = \begin{bmatrix} 0 & 0\\ 0 & 0\\ d_{31} & 0\\ d_{41} & 0 \end{bmatrix} \tag{10}$$

where

- States: $x = [\omega_{cp}\ P_{om}\ m_{om}\ P_{sm}\ m_{sm}\ m_{H_2}\ m_{w,an}\ m_{N_2}\ m_{O_2}\ T_{st}]^T$.
- Inputs: $u = [I_{st}\ v_{cm}]^T$ where the scheduling variable is I_{st}.
- Outputs: $y = [P_{sm}\ v_{st}\ \lambda_{O_2}\ \omega_{cp}]$.
- Perturbations: $z = [T_{amb}\ P_{atm}]$.

In this case the scheduling variable is the current (I_{st}). Thus Eq. (6) is $\tilde{\vartheta}_k = f(I_{st,k})$ and the varying parameters (a_{ij}, b_{ij}, c_{ij} and d_{ij})

of the system matrices. Consequently the system in Eq. (9) can be particularized as follows.

$$\begin{aligned}\mathbf{x}_{k+1} &= \sum_{j=1}^{N}\alpha^j(I_{st,k})\cdot[\mathbf{A}_j(\vartheta^j)\quad \mathbf{B}_j(\vartheta^j)]\cdot\begin{bmatrix}\mathbf{x}_k\\ \mathbf{u}_k\end{bmatrix},\\ \mathbf{y}_k &= \sum_{j=1}^{N}\alpha^j(I_{st,k})\cdot[\mathbf{C}_j(\vartheta^j)\quad \mathbf{D}_j(\vartheta^j)]\cdot\begin{bmatrix}\mathbf{x}_k\\ \mathbf{u}_k\end{bmatrix}.\end{aligned} \tag{11}$$

4. Linear parameter varying observer

4.1. Definition

Using the PEMFC LPV model obtained in previous section, a discrete time LPV observer for state estimation with *Luenberger observer* structure can be expressed as

$$\begin{aligned}\hat{\mathbf{x}}_{k+1} &= \mathbf{A}(\tilde{\vartheta}_k)\hat{x}_k + \mathbf{B}(\tilde{\vartheta}_k)\mathbf{u}_k + \mathbf{L}(\tilde{\vartheta}_k)(\mathbf{y}_k - \hat{\mathbf{y}}_k) + \mathbf{w}_k,\\ \hat{\mathbf{y}}_k &= \mathbf{C}(\tilde{\vartheta}_k)\hat{\mathbf{x}}_k + \mathbf{D}(\tilde{\vartheta}_k)\mathbf{u}_k + \mathbf{v}_k.\end{aligned} \tag{12}$$

Using Eq. (11) the observer can be alternatively expressed as

$$\begin{aligned}\hat{\mathbf{x}}_{k+1} &= \sum_{j=1}^{N}\alpha^j(I_{st,k})[\mathbf{A}_j^o(\vartheta^j)\quad \mathbf{B}_j(\vartheta^j)]\cdot\begin{bmatrix}\hat{\mathbf{x}}_k\\ \mathbf{u}_k\end{bmatrix},\\ \hat{\mathbf{y}}_k &= \sum_{j=1}^{N}\alpha^j(I_{st,k})[\mathbf{C}_j(\vartheta^j)\quad \mathbf{D}_j(\vartheta^j)]\cdot\begin{bmatrix}\hat{\mathbf{x}}_k\\ \mathbf{u}_k\end{bmatrix},\end{aligned} \tag{13}$$

where

$$\mathbf{A}_j^o = \mathbf{A}_j(\vartheta^j) - \mathbf{L}_j(\vartheta^j)\cdot\mathbf{C}_j(\vartheta^j).$$

The observer gain ($\mathbf{L}$) should be designed to guarantee closed loop stability for all operating points, i.e. $\tilde{\vartheta}_k \in \Theta$. This is achieved through LMI formulation for pole-placement within a wide class of pole clustering regions, defined by an affix $(-q, 0)$ and a radius r such that $(-q+r)<0$ [22].

4.2. Observability analysis

The observer design implies the fulfilment of the observability condition that is related to the number of states that can be inferred (or estimated) based on the available measured outputs. For the study of the system observability degree at each operating point (ϑ) the following conditions are used

$$\text{rank}\left(\begin{bmatrix}\lambda_i I - \mathbf{A}\\ \mathbf{C}\end{bmatrix}\right);\qquad \text{cond}\left(\begin{bmatrix}\lambda_i \mathbf{I} - \mathbf{A}\\ \mathbf{C}\end{bmatrix}\right). \tag{14}$$

As discussed in [4], a given system eigenvalue λ_i is unobservable if the rank condition indicates a rank loss. On the other hand, a large condition number implies that the corresponding eigenvalue is weakly observable.

5. Application to fault detection

In order to test the proposed modelling methodology for fault detection, a common set of faults have been selected as benchmark. This set of fault was included in the model (Ballard, Nexa©) [11] in simulation environment in the MATLAB/SIMULINK© (see Fig. 1).

5.1. Model analysis

The stability of the PEMFC system, described in LPV form by Eq. (5), at each operating point is verified if all the eigenvalues of the system are negative. In the case of the a operating point corresponding to I_{st} = 15 A, the stability of the system can be verified by the eigenvalues shown in Table 1. On the other hand, although the system is observable using the observability matrix test, the observability of the system could be further analyzed with conditions showed in Eq. (14).

Table 1
Eigenvalues, rank and condition number for the observability analysis of the polytopic LPV system at I_{st} = 15 A.

State	λ_i	Rank	Cond
ω_{cp}	−1.00E+04	10	1.11E−03
P_{rm}	−543.8	10	27.92
m_{rm}	−388	10	31.87
P_{sm}	−49.9	10	404.82
m_{sm}	−13.14	10	2.22E+03
m_{H_2}	−4.88	10	1.04E+04
m_{an}	−1.72	10	5.23E+04
m_{N_2}	−1.26	10	7.53E+04
m_{O_2}	−0.003	10	1.90E+07
T_{st}	−2.50E−07	10	3.31E+11

Table 2
Eigenvalues, rank and condition number for the observability analysis of the reduced polytopic LPV system at I_{st} = 15 A.

State	λ_i	Rank	Cond
x_1	−26.81	4	30.4
x_2	−4.91	4	11.5
x_3	−2.21	4	88.94
x_4	−3.50E−03	4	3.80E+03

From Table 1, it is clear to see that there are states (ω_{cp}, P_{sm}, m_{sm}, P_{rm}, m_{rm}) which contain fast dynamics compared to others such as the temperature (T_{st}) or oxygen mass (m_{O_2}). Both types of dynamics could decrease the observability performance of the system producing problems with the state estimation using the observer (Table 2). This can be verified by looking at condition number introduced in Eq. (14). To solve this problem, the order of the model should be reduced as proposed in [23]. Table 1 shows that the eigenvalues of the four first states present a higher value than the rest of them. This means that the model can be reduced to a four order state space model instead of the original ten order state space. The reduced system is observable and the condition number has improved with respect to the values presented in Table 3.

In order to test the behaviour of the reduced model compared to the complete model, both models were implemented in simulation. Fig. 3 shows the simulation results of the complete and reduced PEMFC LPV model under a sequents of operating point changes in current demand (I_{st}). This figure shows also the measured outputs for comparison with those generated in simulation. Fig. 4 shows

Table 3
Description of the fault scenarios implemented in FGB.

ID	Fault description	Type	Magnitude
f_1	There is a suddenly increase of friction in the mechanical component part of the compressor	Parametric abrupt	Δk_R = 60%
f_2	Degradation in the stack cells stack is presented because of contact-sensitivity reactions against to a reaction killer	Parametric abrupt	40%
f_3	Hydrogen leak in the anode is presented because of seal degradation.	Parametric abrupt	$A_{nl,f}$ = 2E+2
f_4	A suddenly leak of hydrogen is presented at the anode inlet manifold	Parametric abrupt	80%
f_5	A suddenly leak of air is presented at the inlet outlet supply manifold inlet manifold	Parametric abrupt	10%

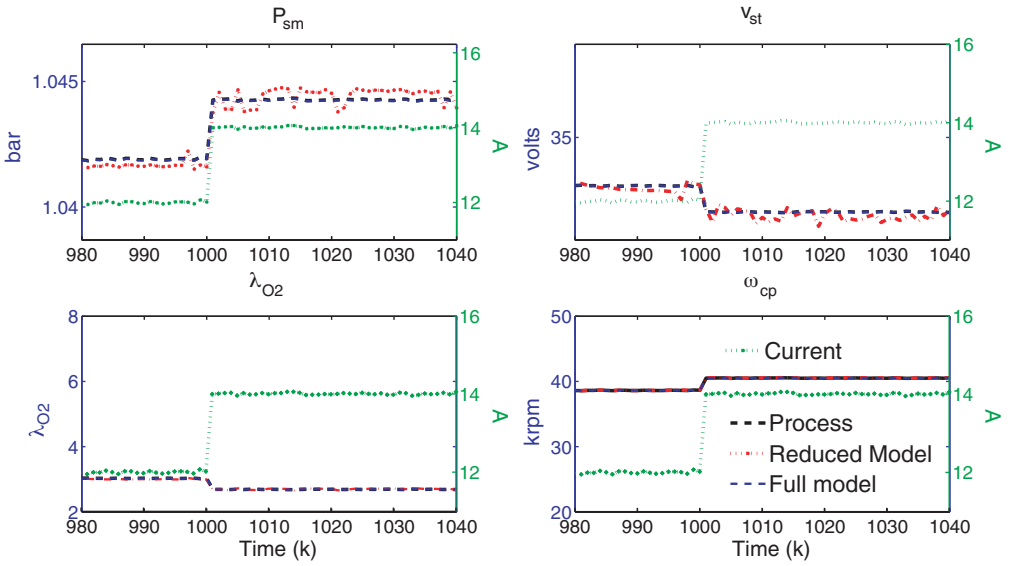

Fig. 3. Comparison of process output signal between real and reduced polytope LPV models.

the model error between the models and the measured outputs of the real process. From either of the two previous figures, it can be noticed that the reduced model presents better performance than the complete one. This result justifies the model reduction since improves the observability and numerical conditioning properties.

5.2. Fault benchmark

The usefulness of LPV model and observer proposed in this paper is illustrated in fault detection. For this purpose, a set of common possible fault scenarios is considered and implemented using the simulator presented in Fig. 1 by adding a fault generator block (FGB) (see Fig. 7). Table 3 describes the set of faults which were considered as case study. In the following section, it is described how the faults were included in simulation.

5.2.1. Fault 1

The fault f_1 is simulated with an increment, ΔR_{cm}, in the compressor motor resistance R_{cm}. The fault effect is translated in a change in the compressor torque τ_{cm} affecting directly the state variable ω_{cp}

$$\tau_{cm} = \frac{\eta_{cm} k_t}{R_{cm} + \Delta R_{cm}} (v_{cm} - k_v \omega_{cm}), \tag{15}$$

where η_{cm} is the motor mechanical efficiency, k_t and k_v are motor constants, and ω_{cm} is the compressor speed. Furthermore, the parameter is related with the state of P_{sm} because its dynamics are governed by the compressor inlet air flow

$$W_{ca,i} = (k_{sm} + \Delta k_{sm})(P_{sm} - P_{cp}), \tag{16}$$

where P_{cp} is the compressor pressure and P_{sm} is the supply manifold pressure. The amount of flow that is feed into the cathode is related

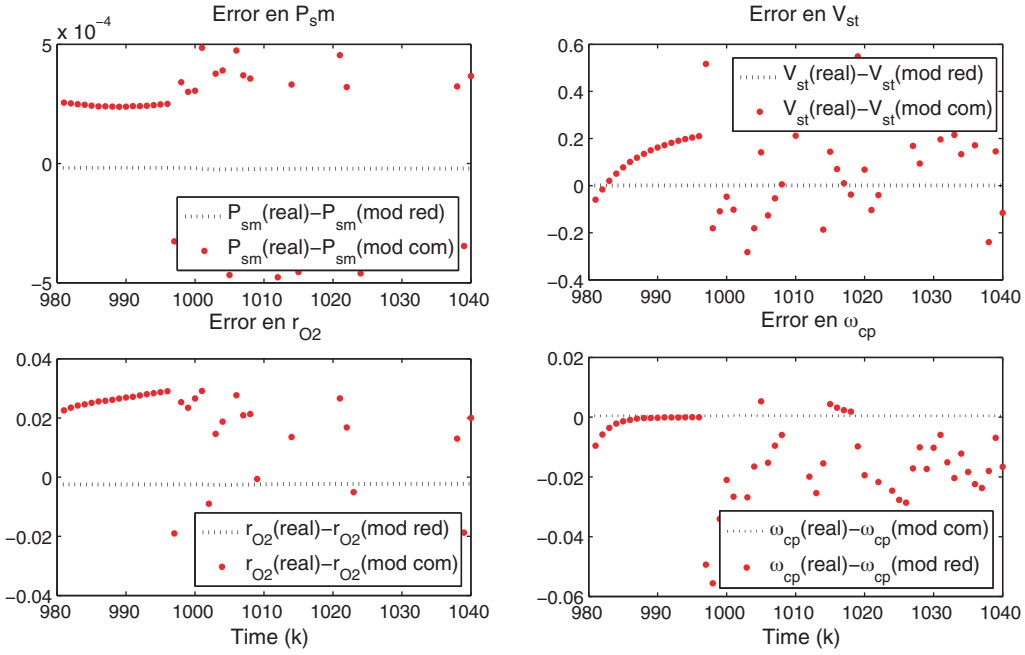

Fig. 4. Model residuals (reduced model and real process data).

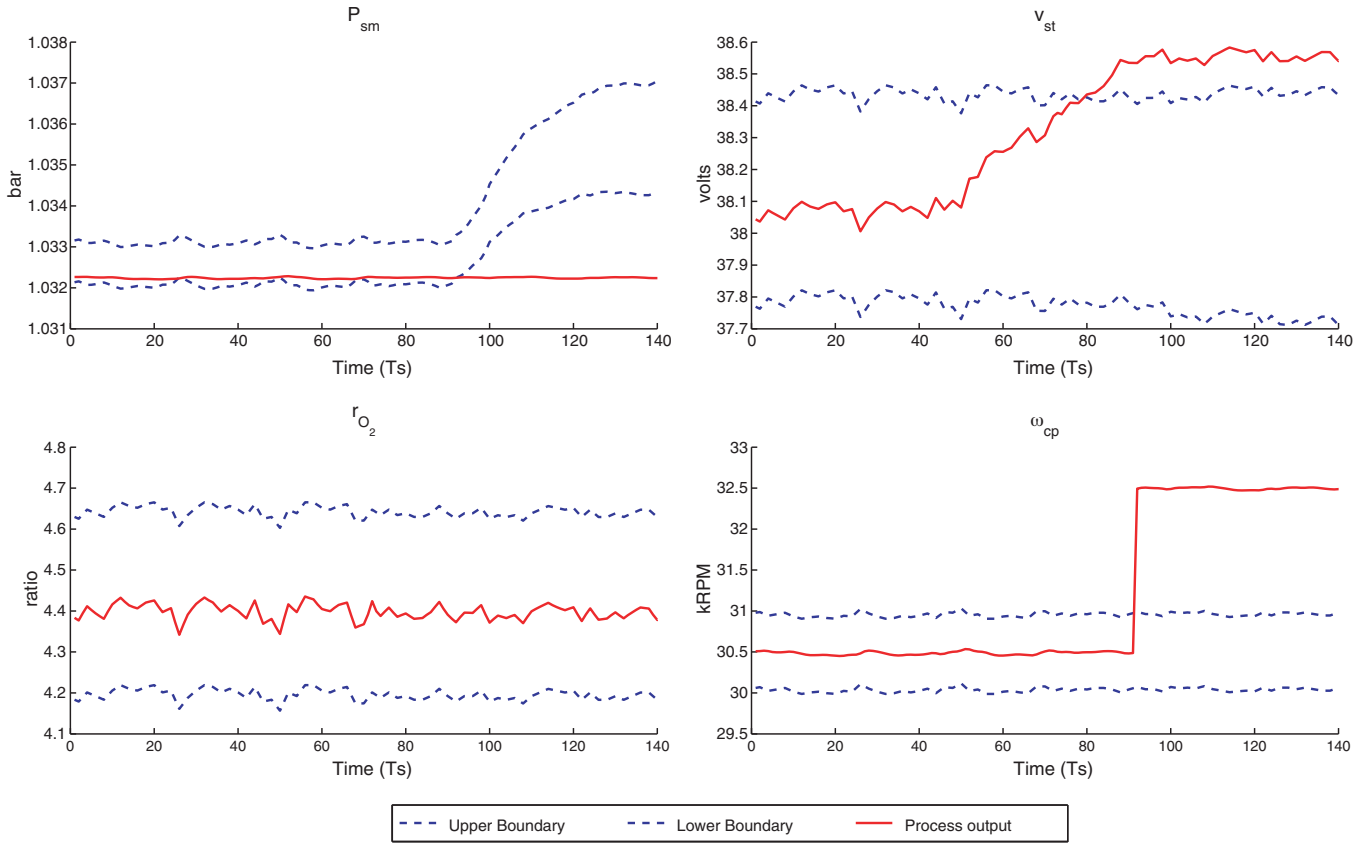

Fig. 5. Confidence intervals for predicted outputs against real measurements in faultily operation (f_2, f_4).

to pressure with a linear constant k_{sm}. It is possible to simulate a reduction in the supply manifold as a change in k_{sm} as Δk_{sm}. Thus, the air mass flow is affected by the fault and consequently, the total mass balance across the PEMFC changes.

5.2.2. Fault 2

Fault f_2 is presented as any contamination in the reaction into the stack reducing the chemical reaction efficiency by decreasing of catalysis active area. The current density, i, is defined as current per area in a single cell, which is equals to stack current I_{st} (A), per cell active area, A_{fc} (cm^2). If the stack is mead of a set of cells in series architecture.

$$i = \frac{I_{st}}{A_{fc} \cdot \Delta A_{fc}}, \tag{17}$$

where ΔA_{fc} is the active contaminated area.

Because of the major voltage drops are associated with current density for non-linear relations, see [24], current density is an important issue for total stack voltage

$$v_{st} = n_{fc} \times [E - v_{act} - v_{ohm} - v_{conc}], \tag{18}$$

where E is the open circuit voltage; v_{act}, v_{ohm} and v_{conc} are activation loss, ohmic loss and concentration loss, respectively, then is clear that fault f_2 will have a direct action over the output of stack voltage.

5.2.3. Fault 3

The term $W_{H_2,nl}$ introduced in Eq. (10) represents the natural leak from the anode of the fuel cell stack. This leak is always present due to the physical stack sealing design. It is assumed that the natural leak is governed by a standard orifice relation through an effective area, A_{nl}. This parameter has been obtained in [25]. In order to simulate a degradation in the seal a change in A_{nl} is used as $A_{nl,f} = A_{nl} f_3$.

$$W_{H_2,nl} = \frac{A_{nl,f} P_{an}}{\sqrt{R_{an}\phi_{an}}} P_r^{1/\gamma} \left(\frac{2\gamma}{\gamma - 1} [1 - P_r^{(\gamma-1)/\gamma}] \right)^{1/2}, \tag{19}$$

where $P_r = P_{an}/P_{atm}$ is the pressure ratio across the assumed leak and the anode gas constant, R_{an}, is calculated through the universal gas constant, R as follows

$$R_{an} = \frac{R}{y_{H_2} M_{H_2} + (1 - y_{H_2}) M_{H_2O}}, \tag{20}$$

where the molar fraction of hydrogen in the anode is given by

$$y_{H_2} = \frac{P_{an} - \phi_{an} P_{sat_{T=st}}}{P_{an}}. \tag{21}$$

5.2.4. Fault 4

This fault introduces a leak of hydrogen and is simulated as a change in the mass balance in the hydrogen inlet flow as follows

$$W_{H_2,f} = W_{H_2,i} - W_{H_2,if_4}. \tag{22}$$

5.2.5. Fault 5

This fault appears as a leak of air at the cathode inlet flow. Because this fault is considered as a leak, it is introduced in the mass balance, as fault f_4, as follows

$$W_{hm,f} = W_{hm,i} - W_{hm,if_5}. \tag{23}$$

Note that the amount of air that does not enter into the system will not only create an abrupt change in the total mass balance, where m_{O_2}, m_{N_2} state variable are mainly involved, but also a system pressure change.

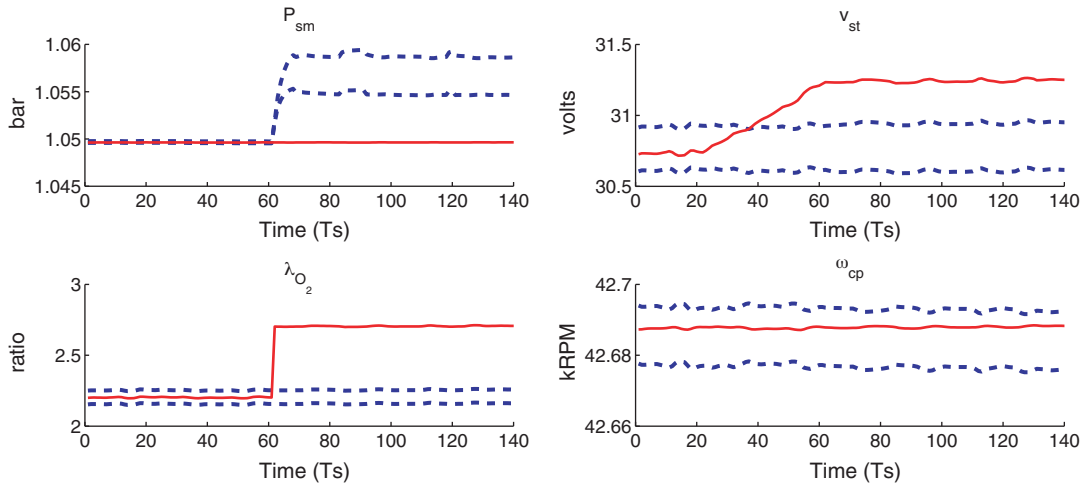

Fig. 6. Confidence intervals for predicted outputs against real measurements in faultily operation (f_2, f_4).

5.3. Fault detection systems

The fault diagnosis system (FDS) based on the LPV observer proposed in this paper has been implemented using MATLAB/SIMULINK environment [26]. The simulator of fuel cell model (Ballard Nexa©) presented in Section 2.1 is used as virtual reality for the fault detection case study. The FGB and FDS subsystems blocks were added to the PEM FC simulator to create the fault scenarios presented in the previous section.

5.3.1. Fault detection process (FDP)

Using the measured inputs and outputs presented in Section 2.1 and using the structural analysis methodology [27], the following set of residuals can be obtained as:

$$\begin{aligned} r_1 &= P_{sm} - \hat{P}_{sm}, \\ r_2 &= \omega_{cp} - \hat{\omega}_{cp}, \\ r_3 &= \lambda_{O_2} - \hat{\lambda}_{O_2}, \\ r_4 &= v_{st} - \hat{v}_{st}. \end{aligned} \tag{24}$$

The residuals are defined conceptually as the differences the process measurements and output estimation from the LPV observer as described in Section 3.2. From the model analysis in Section 5.1, the reduced model offers a better performance when implementing the LPV observer than the complete model. Thus the reduced model is used for creating the PEMFC LPV model.

Fig. 5 shows the measured and the confidence intervals for predicted outputs considering noise and process noise. Notice that when the f_2 is introduced at $k = 50$ in the PEMFC system, at the time $k = 85$ the sensor measurements cross the boundaries of confidence intervals of predicted outputs. This allows detecting the fault.

Fig. 6 shows PEMFC process behaviour compared with the adaptive thresholding generated the interval observer. The process suffers a degradation in supply pressure (P_{sm}) sensor fault over the time starting from $k = 20$ and ends in $k = 60$, the measurement cross the upper boundary at $k = 40$. Note that the other variables do not cross their thresholds. Later appears a sensor offset in λ_{O_2}, that leads the measurement to cross the upper bound at $k = 60$. The effect of this second fault additionally acts over the interval estimation of ω_{cp} (Fig. 7).

The confidence intervals for predicted outputs are computed using zonotope-based algorithm proposed in [28], which offers an efficient way of taking into account model uncertainty when estimating the state using an LPV observer.

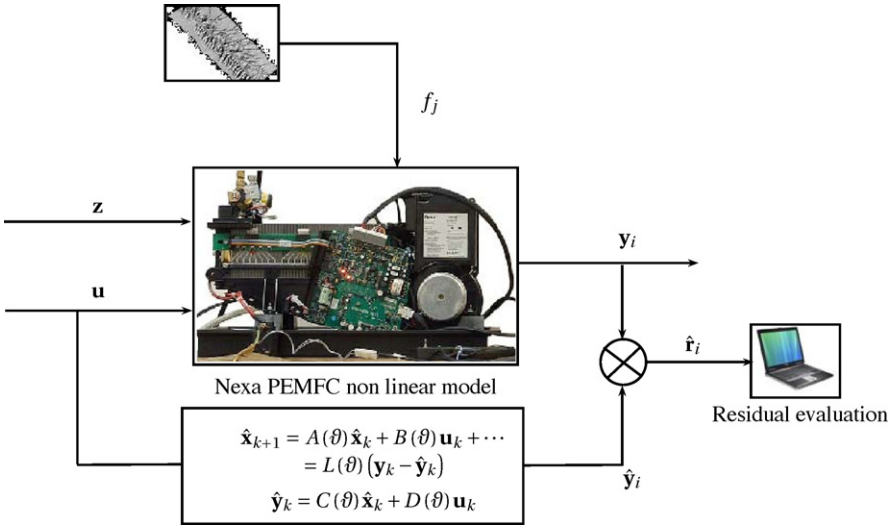

Fig. 7. Fault generator block (FGB) and fault diagnosis system (FDS) implementation diagram.

6. Conclusions

In this paper, an LPV model is introduced as a means to approximate a PEMFC that presents a highly non-linear behaviour using a model with linear structure but with parameters that vary with the operating point. This model can be obtained from the linearization of non-linear model which has been calibrated above a set of data from a commercial PEMFC model (Ballard, Nexa©) around a set of operating points. In addition to the LPV model, the paper proposes the design of an LPV observer to estimate PEMFC system states. To illustrate the usefulness of the LPV model and observer, the application to fault detection is used. The paper also analysis the observability of the LPV model obtained concluding that the complete LPV model contains dynamics that are very different that create numerical difficulties in the observation implementation. These difficulties can be overcome by model reduction neglecting system fast dynamics. The application of the LPV observer to fault detection is shown using a simulator developed using an experimentally calibrated nonlinear model of a typical PEMFC (Nexa© Power Module). A set of common fault scenarios have been defined and implemented in the simulator to test the LPV observer in fault detection. Finally, the paper presents how the observer can satisfactorily detect faults in some of the fault scenarios defined. As an extension of the research presented in this paper, an algorithm that allows not only detect faults but also isolate them is being developed based also in the LPV observer developed. Some preliminary results have already been obtained that show promising results in this line.

References

[1] D. Feroldi, M. Serra, J. Riera, Journal of Power Sources 169 (2007) 205Ű–212Ű.
[2] T. Escobet, D. Feroldi, S. de Lira, V. Puig, J. Quevedo, J. Riera, M. Serra, Journal of Power Sources (2009) 205–212.
[3] J. Pukrushpan, H. Peng, A. Stefanopoulou, Journal of Dynamics Systems, Measurement, and Control 126 (2002) 14–25.
[4] T. Pukrushpan, A.G. Stefanopoulou, Automotive Research Center, Department of Mechanical Engineering 126 (2004) 14–25.
[5] P. Apkarian, P. Gahinet, IEEE Transactions on Automatic Control 40 (1995) 853–863.
[6] P. Falugi, L. Giarre, L. Chisci, G. Zappa, in: IFAC Workshop on Periodic Control Systems, 2001, pp. 33–38.
[7] J.S. Humbert, A.J. Krener, International Journal of Control 71 (1998) 805–821.
[8] J.S. Shamma, M. Athans, Automatica 27 (1991) 559–564.
[9] J. Shamma, Linearization and Gain Scheduling, W. Levine Control Handbook, CRC Press Edition, Boca Raton, 1996.
[10] J. Shamma, D. Xiong, Automatica 35 (1999) 1081–1089.
[11] S. de Lira, V. Puig, J. Quevedo, National Congress of Fuel Cells, CONAPICCE, Sevilla, Spain, 2010.
[12] D. Marquardt, SIAM Journal Applied Mathematics 11 (1963) 431–441.
[13] J. Dennis, Nonlinear Least-Squares: State of the Art in Numerical Analysis, D. Jacobs ed., Academic Press, 1977, pp. 269–312.
[14] C. Mehendale, M.G. Karolos, American Control Conference, 2006, pp. 14–16.
[15] L. Fabien, Z. Jing-Yun, P. Borne, Communications & Control 1 (2006) 73–84.
[16] C. Mehendale, M.G. Karolos, 43rd IEEE Conference on Decision and Control, Atlantis, Paradise Island, Bahamas, 2004, pp. 14–17.
[17] P. Barahyi, D. Tikk, Y. Yam, R. Patton, From differential equations to PDC controller design via numerical transformation, Computers in Industry 51 (2003) 281–297.
[18] B. Bamieh, L. Giarre, Identification for linear parameter varying models, the 38th IEEE Control and Decision Conference, 2 (1999) 1505-1510.
[19] B. Bamieh, L. Giarre, Identification For a General Class of LPV Models, the IFAC systemidentification (2000).
[20] B. Bamieh, L. Giarre, Identification for a General Class of LPV Models, the IFAC System Identification, 2000.
[21] B. Bamieh, L. Giarre, International Journal of Robust and Nonlinear Control 12 (2002) 841–853.
[22] M. Chilali, P. Gahinet, IEEE Transactions on Automatic Control 41 (1996) 358–367.
[23] R Moore, Interval Analysis, Prentice-Hall, Englewood Cliffs, 1966.
[24] J. Larminie, A. Dicks, Fuel Cell Systems Explained, John Wiley & Sons Inc., 2003.
[25] A. Ingimundarson, A.G. Stefanopoulou, D.A. McKay, IEEE Transactions on Automatic Control 16 (2005) 1004–1012.
[26] C. Spiegel, PEM Fuel Cell: Modeling and Simulation Using MATLAB, Elsevier, 2008.
[27] M. Blanke, M. Kinnaert, J. Lunze, M. Staroswiecki, Diagnosis Fault-tolerant Control, Springer-Verlag, Berlin/Heidelberg, 2003.
[28] S. De Lira, J. Quevedo, V. Puig, 20th International Workshop on Principles of Fault Diagnosis, DX, Stockholm, pp. 91-98.